Heat fluxes measurement on the shocktube wall

© *Yu.V. Dobrov, V.A. Lashkov*

St. Petersburg State University,
199034 St. Petersburg, Russia
e-mail: youdobrov@gmail.com

In this paper we carried out experimental study of a heat flux on the shocktube surface during passage of shock wave using a gradient sensor based on bismuth single crystal. The obtained experimental data were compared with numerical simulation results. It is shown that after passing through contact surface that separating the hot „plug" and pushing gas, the colder gas flow is mixed with the hot one. The heat transfer on the contact surface was evaluated.

Keywords: shock tube, heat flux, non-stationary heat measurements.

Introduction

A well-known tool for studying rapidly changing gas-dynamic processes is a shock tube. Temperature, gas pressure, and, of course, heat fluxes on the wall of the shock tube are nonsteady. In the paper [1], where a gradient heat flux sensor based on crystalline bismuth was used, it is noted that different mechanisms of heat transfer apparently exist on the side and end walls of the shock tube channel. The experiment [2] showed that at the end of the shock tube channel, when the shock wave is reflected, the heat flux density in the initial period, the duration of which is approximately 1 ms, gradually increases to a certain constant level. These experimental data contradict the results of theoretical studies. A rigorous analysis of the gas flow parameters in the boundary layer, which is specified on the wall during the passage of a shock wave, can be found in [3]. The difference between the experimental data [1,2] and the theoretical ideas [3] required an identification of the reason for this discrepancy.

In an experimental study [4], the heating of the shock tube surface was studied depending on the intensity of the passing shock wave and the effect of heat transfer on the transition from laminar to turbulent flow behind the shock wave was analyzed. It is shown that with an increase in the differential pressure and, accordingly, the velocity of passage of the shock wave, the heating of the surface of the shock tube also increases. The transition to the turbulent flow regime behind the shock wave and the increase in the intensity of heat transfer on the pipe wall with a change in the flow regime are also shown, and the length of the laminar zone is estimated. Film thermal sensors based on a colloidal paste of chloroplatinic acid mounted on a glass substrate were applied in this paper.

A review of the researches dedicated to studying of the boundary layer after the shock wave disturbance and the heat flux on the wall can be found in [5]. In this paper

to measure rapidly changing heat fluxes the ALTP heat flux sensor was applied, which has a time resolution of the order of $1\,\mu$s and is applied for the direct measurements of the heat flux on the wall.

Special interest in measuring temperature and heat fluxes is associated with an increase in flight speed and the interaction of high enthalpic gas flotation with the surface of an aerodynamic body. This is the reason for the emergence of new means and methods for measuring heat fluxes, which have a high space-time resolution. In the paper [6], measurements of the heat flux during the reflection of a shock wave from the end of the shock tube and during the external supersonic gas flow around the model using a sensor on anisotropic elements were carried out. The results of these measurements were compared with the readings of a thin-film resistance sensor. The comparison showed the correctness and applicability of the proposed signal processing technique from the sensor on anisotropic elements. The paper [7] presents the opportunity of using high-resolution infrared thermography to visualize nonsteady thermal fields in the study of high-speed heat fluxes from the walls of a shock tube during the shock wave disturbance.

The experimental study of the heat flux dynamics on the surface of a shock tube was carried out in this paper. The main objective of the research was to obtain additional experimental data on the heat flux on the wall of the shock tube using a gradient sensor based on crystalline bismuth and compare them with those presented in the scientific literature, as well as to obtain new data on the change in heat flux when passing through the contact surface. The analysis of opportunity of using a heat flux sensor to measure rapidly changing heat fluxes was carried out. A series of experiments was carried out, during which the position of the heat flux sensor was changed along the length of the shock tube. The values of the heat flux density during the front of the main and reflected shock

waves disturbance were obtained. Numerical modeling of the process was carried out. The obtained experimental data were analyzed taking into account the results of calculations of the gas temperature distribution. It is shown that in the boundary layer there is a mixing of the cold gas following the contact surface with the hot gas left after the passage of the „plug", and estimates of heat transfer on the contact surface are given.

1. Results of the experimental study of the heat flux on the wall of the shock tube

To measure heat fluxes, new types of sensors based on the transverse Seebeck effect [8], which is determined by the generation of EMF in an anisotropic medium in the direction perpendicular to the temperature gradient [9], are widely used. These sensors attract attention with their high sensitivity and speed [10]. Gradient heat flow sensors (GHFS) can operate in a wide range of heat flows and temperatures.

The heat fluxes were measured on a shock tube made of aluminum alloy D16 (Fig. 1). Air was used as the working and driving gases in the experiments. The shock tube consists of a low-pressure 1 chamber, from which air was evacuated using a vacuum pump, and a high-pressure 2 chamber, which is under atmospheric pressure. The tube diameter is 33.5 mm. The length of the atmospheric part of the tube is 0.5 m, the length of the low-pressure chamber is $L_x = 2.11$ m. The diaphragm 3 made of polyethylene film with a thin metallized layer separating the atmospheric and low-pressure chambers was mechanically torn using a special knife 4 when the pressure in the low-pressure chamber reached a predetermined level.

When the diaphragm ruptured, a shock wave propagated through the low-pressure tube, the velocity of which was recorded using piezoelectric pressure sensors installed at a known distance from each other. The shock voltage coming from the piezoelectric sensor served as a signal to start recording the signal from the GHFS 5. The heat flow sensor was installed on the cylindrical surface of the tube at different distances L_d from its end, as well as at the very end of the tube.
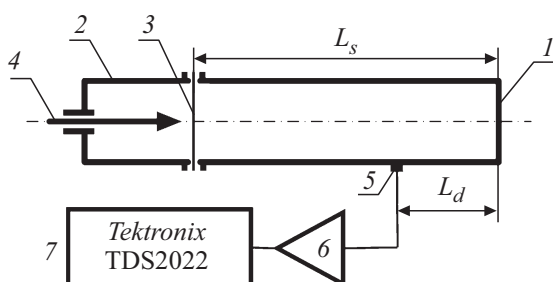

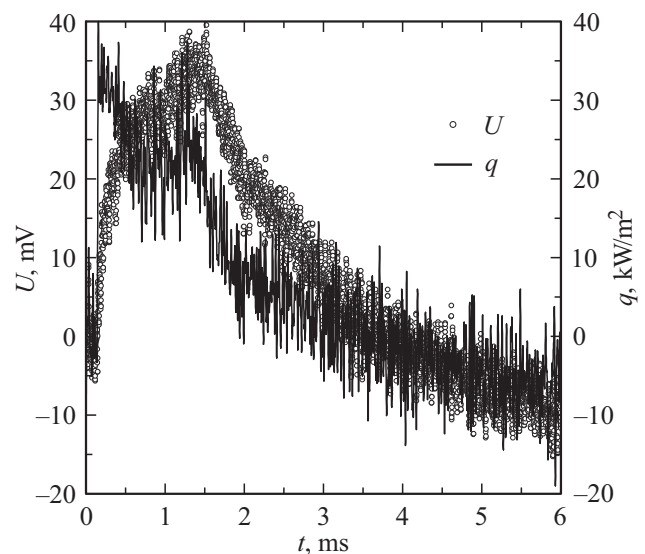**Figure 1.** Shock tube diagram.

Figure 2. Heat flux measurements at a distance of 1.04 m from the end of the shock tube: U — readings of the GHFS, q — heat flux density, t — time.

In this paper the GHFS manufactured at Peter the Great St. Petersburg Polytechnic University was applied, in which high-purity anisotropic bismuth single crystals [11] were used. The sensor is small in size and consists of 10 thermocouples. Its front surface is a square with a side of 2 mm. The transverse dimensions of the thermocouple are 0.2×0.2 mm. The factor of volt-watt sensitivity of the GHFS is equal to 2.4 mV/W.

The signal from the GHFS was fed to an amplifier 6 with a bandwidth of up to 10 MHz and the amplification constant of 175. The result of the heat flux measurement was recorded on an electronic oscilloscope 7 (Tektronix TDS2022). The registered signal was entered into the computer for further processing according to the [12] method.

Figure 2 shows typical readings U of the sensor on the wall of the shock tube when it is located at a distance $L_d = 1.04$ m from the end of the shock tube, as well as the result of sensor signal processing — heat flux density q.

The ratio of pressures on the diaphragm at the moment of its breakthrough is 0.05. The Mach number of the shock wave is M = 1.76. The initial temperature in the low pressure chamber is 293 K, the pressure is 5,000 Pa. The error in determining the shock wave velocity does not exceed 3.5%. There was good repeatability of the measurement results. After processing the measured data, there was an increase in oscillations in the heat flow data. The shock wave disturbance time through the sensor was approximately 5 μs, so the results were smoothed over the 5 μs kernel. Of course, this leads to a decrease in the temporal resolution of the heat fluxes under study.

At the time 0.2 ms (Fig. 2), the front of the primary shock wave arrives at the sensor, followed by a hot „plug". The gas temperature in the „plug" is higher than the initial air

temperature. At the front of the shock wave, the GHFS registers a sharp increase in the heat flux. Then the contact surface comes to the sensor (for approximately 1.5 ms), behind which the driving gas moves. Let us note that there is not such a sharp change in the heat flux when passing through the contact surface.

Assessments made according to the theory of an ideal shock tube show that the temperature of the gas in the hot plug rises by 147 K, and after passing through the contact surface it drops by 105 K relative to the initial temperature. The contact surface comes to the sensor 1.34 ms after the shock wave front. The driving gas has a temperature lower than the initial air temperature and the pipe wall temperature, so the heat flux changes its sign from positive to negative.

It can be noted that the front of the heat flux density during the shock wave disturbance after signal processing is quite sharp. No such voltage change was observed in the initial signal of the sensor. The movement of the contact surface along the sensor changes the positive heat flux to negative very smoothly, the heat flux changes its direction. Moreover, the time during which the value of the heat flux falls is much longer than $5\,\mu$s. The value of the heat flux passes through the zero value in 2.5 ms after the arrival of the contact surface.

In this study, to estimate the nature of the flow in the boundary layer during the passage of a shock wave and to determine the Reynolds number of the transition from a laminar flow regime to a turbulent one, the [5] method was used. For the experiments performed, the dimensional Reynolds number was $\mathrm{Re}_{unit} \approx 1.87 \cdot 10^6$ 1/m. The laminar flow regime is characterized by the constancy of the criterion $\mathrm{St}\sqrt{\mathrm{Re}} = \mathrm{const}$, where St — Stanton
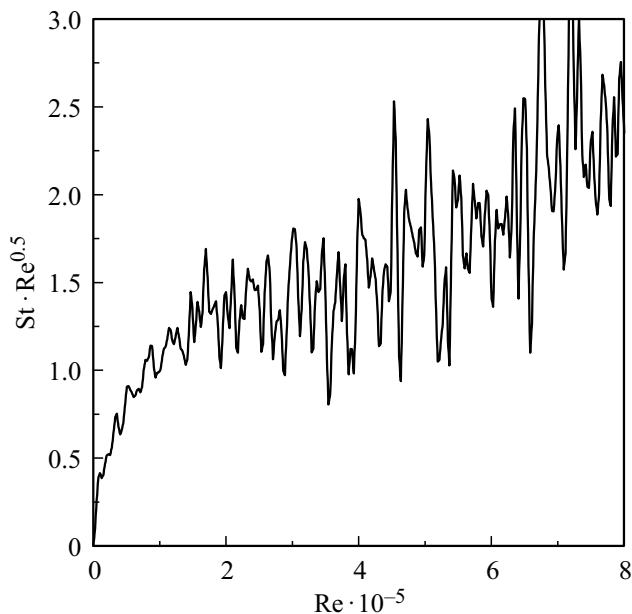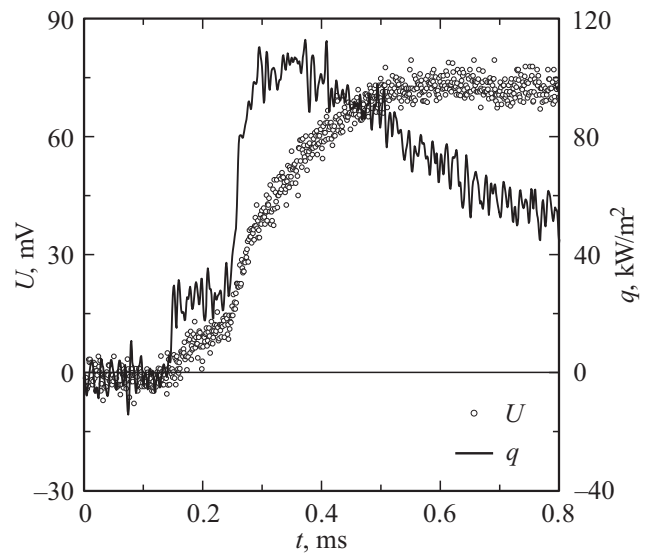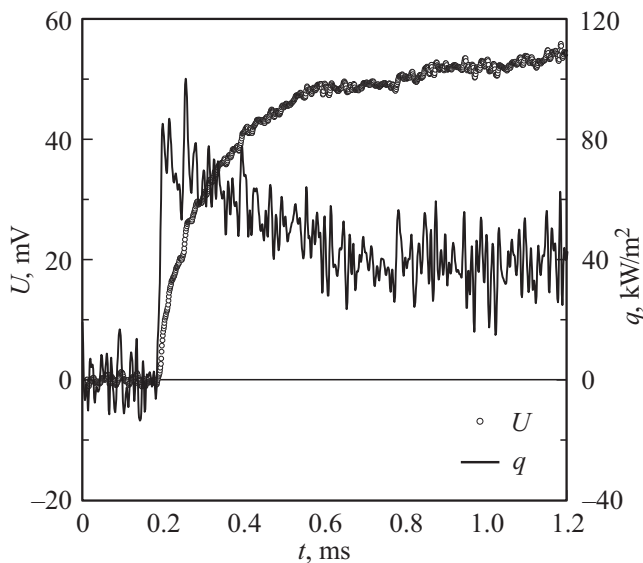

Figure 4. The result of heat flux measurements at a distance of 20 m from the end of the tube: U — readings of the GHFS, q — heat flux density, t — time.

number, Re — Reynolds number, determined from the gas parameters after the shock wave.

Figure 3 shows the behavior of the $\mathrm{St}\sqrt{\mathrm{Re}}$ criterion. The area of its constant value can be noted. At the initial stage, as the Reynolds number increases, the criterion grows to a certain value, approximately $\mathrm{St}\sqrt{\mathrm{Re}} \approx 1.3$. This value is approximately 1.5 times higher than the results of studies given in the paper [4]. The smooth initial growth of the criterion, apparently, can be explained by the fact that the passage of the shock wave through the GHFS takes rather a long time, as was indicated, approximately $5\,\mu$s. Then there is a plateau up to the Reynolds numbers $\mathrm{Re} \approx 5 \cdot 10^5$. Then the growth of the criterion begins, which, apparently, characterizes the beginning of the transition to the turbulent flow in the boundary layer.

In Figure 4 there are readings of the sensor U at a distance $L_d = 20\,\mathrm{mm}$ from the end of the tube, as well as the result of processing the experimental data (heat flux density q). Experimental conditions: Mach number is 1.75, pressure in the low pressure chamber is 4737 Pa. First, a primary shock wave arrives at the sensor — the first sharp increase in the heat flux, which occurs by approximately $150\,\mu$s, (Fig. 4). The air temperature after the shock wave increases by 147 K, which is reflected in an increase in the heat flux.

As the gas passes behind the shock wave, the heat flux changes slightly and remains almost constant. At $250\,\mu$s, the shock wave reflected from the blind end of the tube arrives at the sensor. It increases the gas temperature even more (by approximately 312 K), so the heat flux also increases sharply. Then there is a decrease in the heat flux. The heat transfer conditions change, since the gas behind the primary and reflected shock waves has a different character of motion. As a result of heat transfer between the walls of

Figure 3. Dependence of the criterion $\mathrm{St}\sqrt{\mathrm{Re}}$ on the Reynolds number Re when the shock wave passes at a distance of 1.04 m from the pipe end.

Figure 5. Heat flux measurement at the end of the shock tube: U — readings of the GHFS, q — heat flux density, t — time.

the tube and the gas heated after the reflected shock wave, its temperature decreases, which leads to a drop in the heat flux. Assessment of the criterion for the time interval of the primary shock wave passing through the sensor (for approximately $100\,\mu$s) showed that $\mathrm{St}\sqrt{\mathrm{Re}}$ has a constant value, of $0.9-1.2$.

The heat flux on the end wall of the shock tube was measured. The pressure in the low pressure chamber is $5,380\,$Pa, the Mach number of the shock wave is 1.74. In this case, it can be assumed that the shock wave arrives simultaneously over the entire surface of the sensor. The research results are shown in Fig. 5. The initial GHFS signal is similar to the one observed in the paper [2]. Signal processing according to the [12] method satisfactorily restores the nature of the change in the heat flux density.

According to the theory of an ideal shock tube, the temperature behind the reflected shock wave in this case is $312\,$K higher than the initial temperature of the gas. The researches have shown that after the shock wave is reflected from the end of the tube, the heat flux density increases sharply, but does not remain constant, and subsequently decreases monotonically, which is associated with the transfer of heat from the hot gas to the walls of the shock tube. Similar results were obtained in [13] at higher Mach numbers of the shock wave.

Numerical studies of the heat transfer of a viscous gas after the reflection of a shock wave from the pipe wall are presented in the paper [14]. The case when the Mach number of the primary wave $M = 2$ is reviewed. It is shown how the temperature and heat flux on the tube wall change when it interacts with a primary shock wave ([14], Fig. 3). It is noted that the process of formation of the reflected shock wave is largely due to the thermal regime of the wall.

If the dimensionless thermal activity ε of the wall material is high ($\varepsilon \geq 10^3$), where $\varepsilon = \sqrt{c_t \rho_t \lambda_t \frac{\rho_0 T_0^2}{\mu_0 p_0^2}}$, c — heat capacity, ρ — density, λ — thermal conductivity, μ — viscosity, T — temperature, p — pressure; the index t refers to the wall material, the index 0 — to the initial parameters of the gas, then the time functions of the temperature at the phase boundary and the heat flux density from the gas to the wall are practically independent of the value ε. It is shown that at the initial stage the dimensionless heat flux density $\frac{q_w}{p_0}\sqrt{\frac{\rho_0}{p_0}}$, where q_w — heat flux density into the wall, sharply increases from 0 to 12.5. This occurs in approximately dimensionless time $t_r = \frac{t p_0}{\mu_0} = 6$, and then decreases monotonically with increasing time. The passage of peak values of the heat flux at a level of 0.5 from the maximum lasts approximately 5 units of dimensionless time.

For the conditions of the presented experiments, when the shock wave interacts with the bismuth wall, the dimensionless thermal activity can be determined by the value $\varepsilon \approx 10^4$, and the dimensionless unit of time corresponds to the physical real time $3 \cdot 10^{-9}\,$s The heat flux density was measured at a frequency of $1\,$MHz, i.e. the time between measurements was 2 orders of magnitude longer than the characteristic time of change in the peak values of the heat flux; therefore, a burst in the value of the heat flux density was not registered in the experiments. It can be noted that in the experiments [4] using an ALTP sensor, where the measurement frequency was $40\,$MHz, a burst in the heat flux density is noted when a shock wave passes over the working surface of the sensor ([5], Fig. 8).

## 2. Numerical simulation of gas motion in a shock tube

Numerical modeling was performed in the ANSYS Fluent package. An axially symmetric problem was considered within the model of an ideal viscous gas; the system of Navier−Stokes equations was solved to characterize the gas dynamics:

$$\frac{\partial \rho}{\partial t} + \nabla(\rho \mathbf{V}) = 0,$$

$$\frac{\partial}{\partial t}(\rho \mathbf{V}) + \nabla(\rho \mathbf{V}\mathbf{V}) = -\nabla p + \nabla(\overline{\overline{\boldsymbol{\tau}}}),$$

$$\frac{\partial}{\partial t}(\rho E) + \nabla(\mathbf{V}(\rho E + p)) = \rho q + \nabla(\lambda \nabla T),$$

where ρ is density, $\mathbf{V}$ is the velocity vector, p is pressure, τ is the stress tensor, E is the total energy, the equation of state of Mendeleev−Clapeyron was used, q is the source energy term, λ is the thermal conductivity coefficient, and T is temperature. The Reynolds-Stress Model (RSM) was used to describe the turbulence, since it describes the motion of a viscous gas through simple channels most closely to the available experimental data [15], using the standard near-wall function [16].
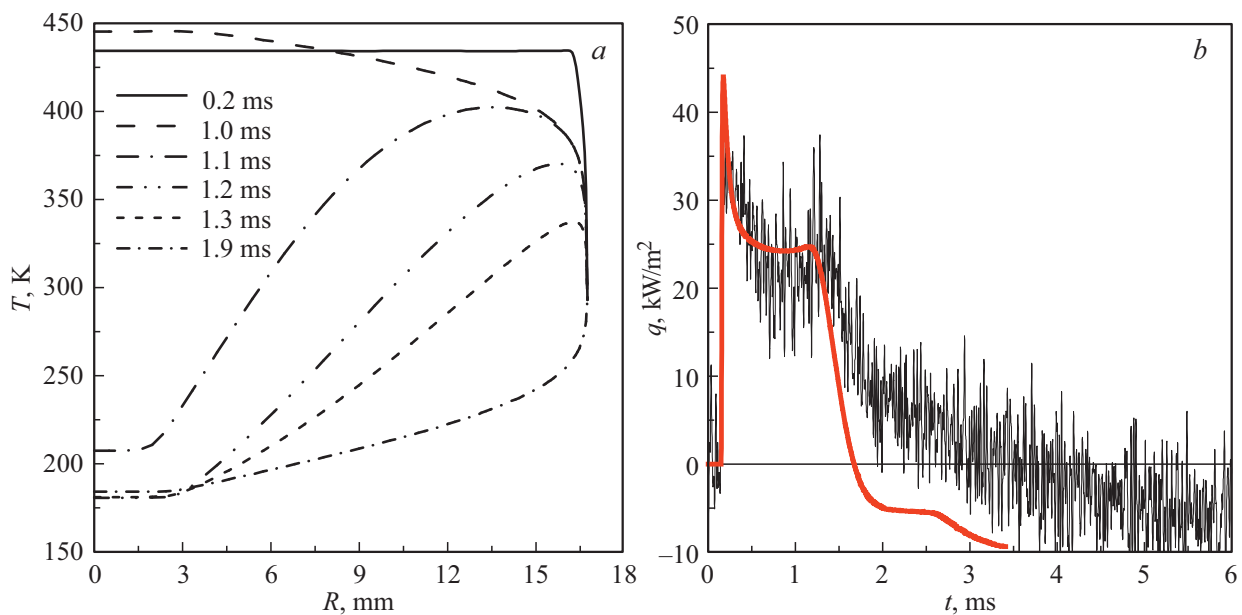
Figure 6. Results of a numerical study of gas parameters during shock wave motion at a distance of 1.04 m from the tube end. *a* — distribution along the radius *R* of the gas temperature *T* pipe (the time corresponding to each temperature distribution is consistent with the time shown in Fig. 6, *b*); *b* — change in heat flux density *q* at different times *t*. Red line (in online version) — calculation, black line — experimental data.

The task was solved under the following initial conditions: in the low pressure chamber — 5000 Pa, in the high-pressure chamber — 101325 Pa, the initial gas temperature — 293 K. According to the calculation conditions, a wall with a constant temperature of 293 K was located at the boundary, since at Mach numbers of the shock wave not exceeding 2, the change in the temperature of the pipe surface does not exceed 5 K [4]. The geometry of the computational domain corresponded to the conditions of the present experiment. The computational grid consists of 412 thousand cells, the grid is exponentially denser towards the wall. The minimum cell size is $5 \cdot 10^{-5}$ m, the maximum value of the wall y+ parameter is 7.35.

Figure 6, *a* presents the results of a numerical study of the gas temperature *T* distribution along the radius *R* at a distance of 1.04 m from the end of the shock tube, where the GHFS was located. The flow temperature distribution along the tube radius for the time instant 0.2 ms corresponds to the distribution observed immediately after the arrival of the shock wave. The distribution related to 1.0 ms shows that the boundary layer is formed and its thickness increases. At approximately 1.1 ms, a contact discontinuity arrives at the sensor: the temperature drops in the flow core, but near the shock tube surface, the velocity profile in the boundary layer remains practically the same as for a time of 1.0 ms. With a further increase in time (1.2, 1.3 ms), the temperature on the flow axis decreases to the temperature of the driving gas, but the temperature near the tube wall remains still higher than the wall temperature (293 K). The temperature profile for time 1.9 ms shows that the temperature distribution near the tube wall changes dramatically: the gas temperature in the

boundary layer becomes lower than the wall temperature: the heat flow direction changes.

Figure 6, *b* shows the results of calculating the heat flux density at a distance of 1.04 m from the end of the shock tube (red line (online version)), which show that there is a sharp increase in the heat flux density, then the value of the heat flux density reaches a certain practically constant level. When passing through the contact surface, the heat flux density decreases, but the falling speed differs from the speed that can be observed when passing through the shock tube. The drop in the value of *q* occurs approximately in a time of 0.2 ms, and the heat flux changes its direction to the opposite. The same Fig. 6, *b* shows the results of an experimental study of the heat flux density (black line). It can be seen that the results of the experiment and the calculation data agree satisfactorily, however, the experiment shows a slower decrease in the heat flux density after passing through the contact surface. This circumstance requires further research.

The passage of the contact surface does not lead to a sharp change in temperature on the flow axis, which is apparently due to the fact that the hot „plug" and the cold driving gas are in contact for a long time and therefore exchange thermal energy. The thermal conductivity of a real gas leads to the fact that a sharp change in temperature on the contact surface „is blurred".

A boundary passes on the contact surface, on both sides of which the gas (in our case, air) has a different temperature. These two areas of the gas, the hot „plug" and the driving cold gas, are in thermal contact, which means that heat exchange should take place between them.

It is possible to assess the change in the temperature of the boundary layers of the gas during the time until the contact surface reaches the location of the heat flux sensor.

The sensor is located at a distance of 1 m from the tube diaphragm. The flow velocity behind the shock wave in our case is $V = 340$ m/s. This means that the time during which the heat exchange takes place is approximately 3 ms.

Let us assume that heat transfer on the tube axis occurs according to the model of a semi-infinite body. The solution for this task, taking into account that there is air on both sides of the contact surface, has the following form [17]:

$$\theta(x, t) = 0.5 \left(1 + erf \left(\frac{x}{2\sqrt{at}} \right) \right),$$

where a — air thermal diffusivity.

It is easy to determine that the thickness of the gas layer on the contact surface, in which the temperature differs from the temperature of the gas in the hot plug and the driving cold gas by more than 1%, is approximately 10 mm. Time of passage of this layer of gas through the heat flow sensor — 30 μs. This time is much shorter than that in numerical calculations. From Fig. 6, a the time of temperature change can be assessed during the passage of the contact surface on the axis as 0.2 ms, which is an order of magnitude longer than the time 30 μs. Obviously, this is due to the fact that the process of heat transfer between gases is influenced not only by the thermal conductivity of the medium, but also by convective heat transfer. Moreover, convective heat transfer undoubtedly depends on the quality of the shock wave formation and the contact surface when the diaphragm breaks. The appearance of large vortices during diaphragm rupture enhances the mixing of hot and cold gases on the contact surface.

The gas temperature in the near-wall layer changes more slowly than in the core of the flow. This process takes approximately 0.8 ms. When a hot „plug“ passes through, a boundary layer is formed on the tube wall. Gas layers located near the tube surface have a flow velocity close to zero. When a cold driving gas arrives, cold layers are superimposed on the hot slow layers. It takes time for the cold and hot layers of gas to mix and exchange energy. This leads to a change in the temperature distribution in the boundary layer and, as a consequence, to a change in the heat flux on the tube wall both in magnitude and direction.

3. Conclusions

An experimental study of the dynamics of heat flow on the wall of a shock tube was carried out using a GHFS based on a bismuth single crystal. Experiments have shown that the used GHFS satisfactorily shows changes in the heat flux on the wall of the shock tube and can be used to study fast thermal processes. It is important to take into account the speed characteristics of the sensor. After using special processing of the GHFS signal, we see a sharp increase in the value of the heat flux density during the passage of the shock wave front.

Based on an experimental and numerical study of the gas flow in a shock tube, it is shown that when passing through the contact surface, the change in the heat flux occurs rather smoothly, which is associated with the mixing of the hot plug gas and the driving gas: in the boundary layer on the tube surface, the cold driving gas mixes with the hot slowly moving layer left after the passage of the plug. On the contact surface in the core of the flow, there is also an exchange of thermal energy between hot and cold gases. Numerical calculations also confirmed that when passing through the contact surface, the heat flux density on the tube wall does not undergo abrupt changes.

Conflict of interest

The authors declare that they have no conflict of interest.

References

[1] S.Z. Sapozhnikov, V.Yu. Mityakov, A.V. Mityakov, R.L. Petrov, V.V. Grigoriev, S.V. Bobashev, N.P. Mende, V.A. Sakharov. Pis'ma v ZhTF, **30** (2), 76 (2004) (in Russian)

[2] S.Z. Sapozhnikov, V.Yu. Mityakov, A.V. Mityakov, S.V. Bobashev, N.P. Mende, V.A. Sakharov. Sovremennaya nauka, **2** (7), 172 (2011) (in Russian)

[3] H. Mirels. *Boundary Layer Research* (Springer, Berlin, Heidelberg, 1957), p. 283−293. DOI: 10.1007/978-3-642-45885-9_22

[4] Yu.A. Polyakov, Yu.V. Makarov. Tekhnologii tekhnosfernoy bezopasnosti, **4** (62), 1 (2015) (in Russian)

[5] H. Knauss, T. Roediger, D.A. Bountin, B.V. Smorodsky, A.A. Maslov, J. Srulijes. J. Spacecraft and Rockets, **46** (2), 255 (2009).

[6] P.A. Popov, V.A. Sakharov, T.A. Lapushkina, S.A. Ponyaev, N.A. Monakhov. Fiziko-khimicheskaya kinetika v gazovoy dinamike, **22** (3), 31 (2021) (in Russian). DOI: 10.33257/PhChGD.22.3.939

[7] I.A. Znamenskaya, A.M. Shagiyanova, E.Yu. Koroteeva, M.I. Muratov, P.A. Ryazanov. Scientific Visualization, **12** (5), 13 (2020). DOI: 10.26583/sv.12.5.02

[8] A.M. Kharitonov. *Tekhnika i metody aerofizicheskogo eksperimenta. P. 2. Metody i sredstva aerofizicheskikh izmereniy* (NGTU, 2007) (in Russian)

[9] A.G. Samoylovich. *Termoelektricheskiye i termomagnitnyye metody prevrashcheniya energii* (Izd-vo LKI, M., 2007), 224 p.

[10] S.V. Bobashev, Yu.P. Golovachov, N.P. Mende, P.A. Popov, B.I. Reznikov, V.A. Sakharov, A.A. Schmidt, A.S. Chernyshev, S.Z. Sapozhnikov, V.Yu. Mityakov, A.V. Mityakov. Tech. Phys. **53** (12), 1634 (2008).
https://doi.org/10.1134/S1063784208120189

[11] S.Z. Sapozhnikov, V.YU. Mityakov, A.V. Mityakov. *Gradiyent-nyye datchiki teplovogo potoka* (SPbGPU, SPb., 2003), 168 p. (in Russian)

[12] Yu.V. Dobrov, V.A. Lashkov, I.Ch. Mashek, A.V. Mityakov, V.Yu. Mityakov, S.Z. Sapozhnikov, R.S. Khoronzhuk. ZhTF, **91** (2), 240 (2021) (in Russian) DOI: 10.21883/0000000000

[13] P.A Popov, V.A Sakharov, S.A Poniaev, N.A Monakhov, M.A Kotov. J. Phys.: Conf. Ser., **1697** (012225), 1 (2020).
DOI: 10.1088/1742-6596/1697/1/012225

[14] P.P. Andreev, Yu.M. Tsirkunov. IFZh, **51** (2), 217 (1986) (in Russian)

[15] A. S. Lubina, A. A. Sedov. *Verifikatsiya CFD-modeley ANSYS FLUENT dlya odnofaznykh techeniy v kanalakh prostoy formy.* 10-ya Mezhdunarodnaya nauchno-tekhnicheskaya konferentsiya „Obespecheniye bezopasnosti AES s VVER" (OKB „GIDROPRESS", Podolsk, Podol'sk, Rossiya, 16−19 maya 2017) (in Russian).

[16] B.E. Launder, D.B. Spalding. Computer Methods in Appl. Mechan. Engineer., **3**, 269 (1974).
DOI: 10.1016/0045-7825(74)90029-2

[17] A.V. Lykov. *Teoriya teploprovodnosti* (Vysshaya Shkola, M., 1967), 600 p. (in Russian)